Simulation of Non-Newtonian Fluid Mixing Using the Lattice Boltzmann Model

JAMES M. BUICK
University of New England
Physics and Engineering
Armidale
NSW
Australia

JOSHUA BOYD
University of New England
Physics and Engineering
Armidale
NSW
Australia

Abstract: This paper investigates the application of the lattice Boltzmann model to non-Newtonian flow simulations in the mixing section of a screw extruder. The non-Newtonian power law model and its implementation into the lattice Boltzmann model are described. Simulation results are presented for a shear thinning fluid. The results show the suitability of the lattice Botlzmann model for performing non-Newtonian simulations of this type. Significant differences are observed between the flow pattern for the shear thinning fluid considered and a Newtonian fluid. This demonstrates the importance of considering the non-Newtonian nature of the fluid in screw extruder simulations.

Key–Words: Screw extruder, non-Newtonian fluid, lattice Boltzmann model

1 Introduction

A single-screw extruder is commonly used in polymer processing and its performance is known to considerably influence the quality and morphology of the final product. For this reason the flow field in the mixing section has been studied by a number of authors to gain a better understanding of the process. Yao *et al.* [1, 2] performed simulations using a finite difference method (FDM) which were found to compare favourably with a visualization experiment involving the flow of high viscosity corn syrup in a rectangular cavity with a moving top boundary. Further work was performed by Horiguchi *et al.* [3] using the lattice gas method (LGM). Their simulations compared favourably with the FDM simulations, visualisation experiments and theory; however a number of small differences were also observed. In particular a small circulation was observed in the bottom left and right corners of the LGM simulations; whereas no circulation is evident in the FDM results. Comparison with theory indicated that the LGM produced a more accurate representation of the flow field relative to the FDM, however a small discrepancy was still observed. Simulations using the lattice Boltzmann model (LBM) were performed by Buick and Cosgrove [4]. The LBM has developed from the LGM and was shown to simulate the flow in the single-screw extruder more accurately and more efficiently than the LGM. Another feature of the LBM is that it is suitable for simulating a non-Newtonian fluid. It has been shown that a non-Newtonian fluid can be simulated with second order accuracy using the LBM with a non-Newtonian viscosity described by a power law model [5].

2 The Lattice Boltzmann Model

The lattice Boltzmann method [6] has recently been developed as an alternative method for simulating a range of fluid flows. LBM simulations are performed on a regular grid defined by Q directional vectors $\mathbf{e}_i$ for $i = 0, 1, ..., Q-1$. At each site, $\mathbf{x}$, each link direction, $\mathbf{e}_i$, has an associated distribution function, $f_i(\mathbf{x}, t)$. The distribution functions interact on the lattice by streaming from one site to a neighbouring site in each time step and by undergoing collisions which are represented by the relaxation of the distribution functions toward their equilibrium. Here we use the D2Q9 lattice which is a two-dimensional lattice with 9 link directions:

$$\mathbf{e}_0 = (0, 0),$$

$$\mathbf{e}_i = \left(\cos\left(\frac{\pi}{2}(i-1)\right), \sin\left(\frac{\pi}{2}(i-1)\right)\right)$$

for i = 1, 2, 3, 4 and

$$\mathbf{e}_i = \sqrt{2}\left(\cos\left(\frac{\pi}{2}(i-1)+\frac{\pi}{4}\right), \sin\left(\frac{\pi}{2}(i-1)+\frac{\pi}{4}\right)\right)$$

for i = 5, 6, 7, 8, see Figure 1.

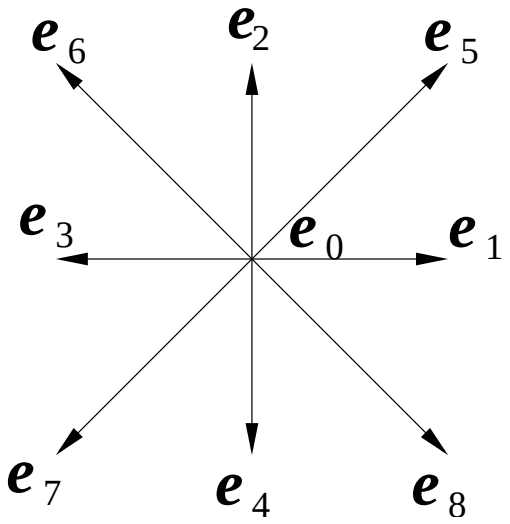

Figure 1: Lattice for the D2Q9 model.

The evolution of the distribution functions on the lattice is governed by the discrete Boltzmann equation [6]:

$$f_i(\mathbf{x}+\mathbf{e}_i, t+1) - f_i(\mathbf{x}, t) = \Omega_i(\mathbf{x}, t). \quad (1)$$

The left-hand side of equation (1) represents the streaming of the distribution functions and the right-hand-side is the relaxation collision operator [6, 7]:

$$\Omega_i = \frac{-1}{\tau}[f_i(\mathbf{x}, t) - f_i^{eq}(\mathbf{x}, t)], \quad (2)$$

where the equilibrium distribution function, f_i^{eq} is determined by a local function of the fluid density, $\rho = \sum_i f_i$ and velocity, $\mathbf{u} = (\sum_i f_i \mathbf{e}_i)/\rho$, [8]

$$f_i^{eq}(\mathbf{x}, t) = w_i \rho (1 + 3\mathbf{e}_i \cdot \mathbf{u} + \frac{9}{2}(\mathbf{e}_i \cdot \mathbf{u})^2 - \frac{3}{2}\mathbf{u}^2) \quad (3)$$

where w_0 = 4/9, w_i = 1/9 for i = 1,2,3,4 and w_i = 1/36 for i = 5,6,7,8. The relaxation time τ is related to the kinematic viscosity ν by

$$\nu = \frac{2\tau - 1}{6}. \quad (4)$$

The LBM reproduces the Navier stokes equation in the nearly incompressible limit and has been shown to be second order accurate in the body of the fluid [6].

2.1 Non-Newtonian Simulations

A non-Newtonian fluid is one where the viscosity is not constant. In such fluids the apparent viscosity can vary with, for example, shear, temperature or time. Here we will consider only shear dependent non-Newtonian fluids. A dialant or shear thickening fluids has an apparent viscosity which increases with increasing strain, for example corn starch, clay slurries and certain surfactants. A psudoplastic or shear thinning fluid has an apparent viscosity which decreases with increasing shear, for example paint and blood [9].

To simulate a shear dependent non-Newtonian fluid, it is necessary to determine the shear at each point in the simulation. This would normally be done by calculating the strain rate tensor:

$$S_{\alpha\beta} = \frac{1}{2}\left(\nabla_\beta u_\alpha + \nabla_\alpha u_\beta\right), \quad (5)$$

where here $\alpha, \beta \in \{x, y\}$. For the LBM, the strain rate tensor can be determined locally as [10]

$$S_{\alpha\beta} = -\frac{3}{2\tau}\sum_i f_i^{neq} \mathbf{e}_{i\alpha}\mathbf{e}_{i\beta}, \quad (6)$$

where $f_i^{neq} = f_i - f_i^{eq}$. Thus the fluid shear can be determined without significant extra computation. The shear rate, $\dot{\gamma}$ is then calculated as

$$\dot{\gamma} = 2\sqrt{D_{II}}, \quad (7)$$

where D_{II} is the second invariant of the strain rate tensor:

$$D_{II} = \sum_{\alpha,\beta=1}^{l} S_{\alpha\beta} S_{\alpha\beta} \quad (8)$$

where here $l = 2$ since we are working in two-dimensions.

Here the apparent viscosity is determined by the power law model [9, 11, 12, 13, 14]:

$$\nu(\dot{\gamma}) = \hat{m}|\dot{\gamma}|^{n-1}, \quad (9)$$

where $\hat{m}$ and n are parameters that are determined by fitting a curve of the form of equation (9) to physical viscometric data.

The parameter n determines the response of the fluid to changes in shear rate, for

$n < 1$, the fluid is shear thinning,

$n = 1$, the fluid is Newtonian, and for

$n > 1$, the fluid is shear thickening.

The non-Newtonian nature of the fluid is modelled by determining the apparent kinematic viscosity $\nu(\dot{\gamma})$ using equations (6)-(9). The relaxation time, τ, corresponding to the apparent viscosity is then determined at each grid point by inverting equation (4).

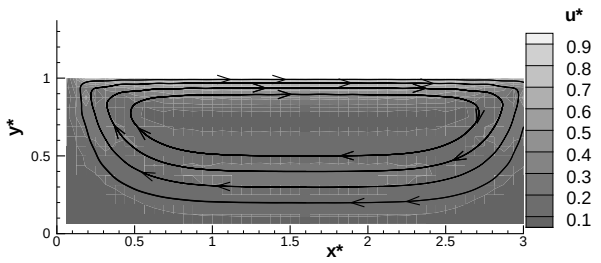

(a) Velocity magnitude and streamlines

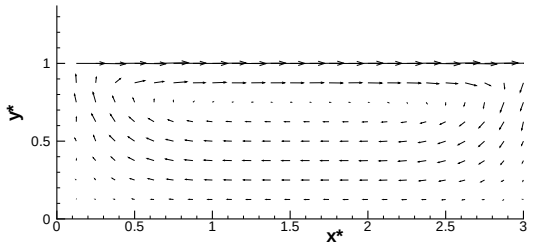

(b) Velocity vectors

Figure 2: Flow pattern in the mixing section for a shear thinning fluid with n = 0.5 (a) shows the magnitude of the dimensionless velocity with streamlines calculated from the flow and (b) the vector field.

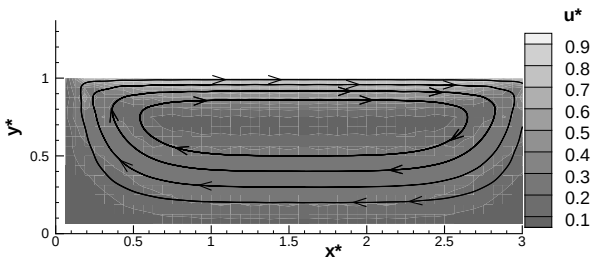

(a) Velocity magnitude and streamlines

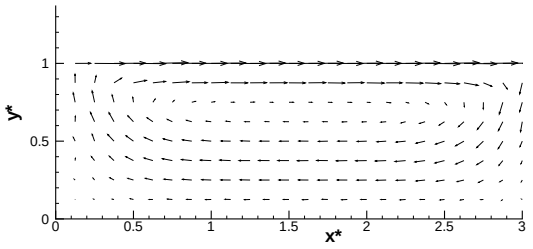

(b) Velocity vectors

Figure 3: Flow pattern in the mixing section for a shear thinning fluid with n = 0.75 a) shows the magnitude of the dimensionless velocity with streamlines calculated from the flow and (b) the vector field.

Equation (9) can be non-dimensionalised and a dimensionless number analogous to the Reynold's number can be defined as

$$Re_{PL} = \frac{U^{2-n}L^n}{\hat{m}} \tag{10}$$

where $\hat{m}$ and n are the power law parameters and U and L are characteristic velocity and length scales respectfully.

2.2 Simulations

Simulations of a single screw extractor were performed using the LBM for a power-law non-Newtonian shear thinning fluid. If the simulation is performed in a frame of reference moving with the rotating screw, the problem reduces to that of a cavity flow with one moving wall and three stationary walls. The velocity can then be separated into a two-dimensional cross-section component and a streamwise component. It is the cross-sectional component, perpendicular to the spiral direction which is considered here. A computational grid of height h and length l was simulated with the top wall at $y = h$ moving with velocity $(u_0, 0)$ and all the other walls stationary. The results are presented in terms of the normalised positions $x^* = x/h$, $y^* = y/h$ and velocities, $(u^*, v^*) = (u/u_0, v/u_0)$.

3 Results and Discussion

Figures 2 and 3 shows the results of simulations using power law models with n = 0.5 and n = 0.75 respectively (that is for shear thinning fluids). Both fluids show the same basic flow pattern as was observed for a Newtonian fluid [4]. However, both flow differ significantly with respect to each other and also with respect to the Newtonian case [4]. The changing flow patterns can most easily be characterised in terms of the y position where the horizontal velocity, u is zero. Comparing Figures 2 and 3 we observe that the region of zero horizontal velocity is closer to the moving top boundary for n = 0.5. Thus the region of flow in the same direction as the moving boundary is compressed and the region of reverse flow is increased for the lower value of n (and the increased non-Newtonian nature of

the fluid). The same trend is observed when comparing Figure 3 to the results for a non-Newtonian fluid [4]. The results demonstrate the ability of the LBM to simulate non-Newtonian flows in a screw extruder. Further they indicate that the flow pattern is dependent on the non-Newtonian nature of the fluid and thus that the correct non-Newtonian parameters should be used for the fluid being simulated. Further work is required to investigate the extend of this dependence for common substances and screw extruder geometries.

4 Conclusion

The results demonstrate the suitability of the lattice Boltzmann model for simulating flows involving non-Newtonian fluids in the mixing section of a screw extruder. Results were obtained for a shear thinning fluid which varied significantly from the results for a Newtonian fluid. This indicates that it is important to correctly model the non-Newtonian nature of a fluid when simulating flow in a screw extruder.

Acknowledgements: This work was partially supported by Sigma Xi Grant no 10040015 and the Australian Postgraduate Award (APA); this assistance is gratefully acknowledged.

References:

[1] W. G. Yao, K. Takahashi and Y. Abe, Analytical Study on Flow and Distributive Mixing of a New Type Pin Mixing Section for Screw Extruder, *Int. Poly. Proc.* XI, 1996, pp. 222–227.

[2] W. G. Yao, K. Takahashi, K. Koyama and G. C. Dai, Design of a New Type Pin Mixing Section for a Screw Extruder Based on Analysis of Flow and Distributive Mixing Performance, *Chem. Eng. Sci.*, 52, 1997, pp. 13–21.

[3] H. Horiguchi, K. Takahashi and T. Tokota, Numerical Simulation of the Flow Field in the Mixing Section of a Screw Extruder by the Lattice Gas Automata Method, *J. Chem. Eng. Japan* 36, 1003, pp. 110–113.

[4] J. M. Buick and J. A. Cosgrove, Numerical simulation of the flow in the mixing section of a screw extruder by the lattice Boltzmann model, *Chem. Eng. Sci.* 61, 2006, pp. 3323–3326.

[5] J. Boyd, J. Buick, and S. Green, A second-order accurate lattice Boltzmann non-Newtonian flow model, *J. Phys. A* 39, 2006, pp. 14241–14247,

[6] S. Chen and G. D. Doolen, Lattice Boltzmann method for fluid flows, *Ann. Rev. Fluid Mech.* 30, 1998, pp. 329-364.

[7] P. L. Bhatnagar, E. P. Gross, and M Krook, A model for collision processes in gases. I. Small amplitude processes in charged and neutral one-component systems, *Phys. Rev.* 94, 1954, pp. 511–525.

[8] Y. H. Qian, D. d' Humières, and P Lallemand, Lattice BGK models for Navier-Stokes equation, *Europhys. Lett.* 17, 1992, pp. 479–484.

[9] A. Quarteroni, M. Tuveri, and A. Veneziani, Computational vascular fluid dynamics: problems, models and methods. *Computing and Visualisation in Science* 2, 2000, pp. 163–197.

[10] A. Artoli. *Mesoscopic Computational Haemodynamics*, Technical report, University of Amsterdam, 2003.

[11] A. Quarteroni and A. Veneziani, *Modeling and Simulation of Blood Flow Problems*, In M.-O. Bristeau, G. Etgen, W. Fitzgibbon, J.L. Lions, J. Periaux, and M.F. Wheeler, editors, *Computational Science for the 21st Century*. Wiley, 1997.

[12] F. Gijsen, *Modeling of Wall Shear Stress in Large Arteries*, PhD thesis, Eindhoven University of Technology, 1998.

[13] P. Neofytou and D. Drikakis. Non-Newtonian flow instability in a channel with a sudden expansion, *J. Non-Newtonian Fluid Mech.* 111, 2003, pp. 127–150.

[14] M.A. Hussain, S. Kar, and R.R. Puniyani, Relationship between power law coefficients and major blood constituents affecting the whole blood viscosity, *J. Biosciences* 24, 1999, pp.329–337.